Available online at www.sciencedirect.com
SCIENCE DIRECT
Polymer 47 (2006) 1640–1648
polymer
www.elsevier.com/locate/polymer

Microstructure and properties of polyester-based polyurethane/titania hybrid films prepared by sol–gel process

Yongchun Chen [a], Shuxue Zhou [a], Guangxin Gu [a], Limin Wu [a,b,*]

[a] *Department of Materials Science and the Advanced Coatings Research Center of China Educational Ministry, Fudan University, Shanghai 200433, People's Republic of China*

[b] *College of Chemistry and Materials Science, Hubei University, Wuhan 430062, People's Republic of China*

Received 23 August 2005; received in revised form 18 December 2005; accepted 21 December 2005
Available online 24 January 2006

Abstract

Polyester polyol/titania hybrid resins and their corresponding polyurethane/titania hybrid films were prepared by in situ method via sol–gel process of titanium *n*-butoxide under acidic condition. The effects of the contents and types of titania sol on the microstructure and some mechanical and optical properties of the hybrids were investigated. It was found that introducing titania into the resin could increase some physical properties such as the viscosity of the resin, modulus, T_g, mechanical strength, abrasion resistance, hardness and UV absorbance, but different titania sols obtained from various molar ratios of water to titanium *n*-butoxide had an obvious influence on the microstructure and properties of the hybrid films.

Keywords: Polyester-based polyurethane; Titania; Hybrid

1. Introduction

Titania based organic–inorganic hybrid materials have been extensively studied recently because of combining the balanced properties of organic polymers (e.g. flexibility, ductility, dielectric) and titania (e.g. high thermal stability, strength, hardness, UV absorbance and high refractive index), even acquiring some special or novel properties due to their special microstructures, thus can be potentially used in many fields such as electrical, optical, structural, photoelectrical, nonlinear optical materials, plastics, rubbers, fibers, coatings, inks, etc. [1–8].

These hybrid materials were usually prepared via sol–gel process [9–16]. For examples, Lee and Chen [17] reported the preparation of PMMA/titania hybrid films with 3-(trimethoxysilyl)propyl methacrylate as the coupling agent via in situ sol–gel process. Sarwar and Ahmad [18] prepared titania-aramid hybrid materials using a sol–gel process and aminophenyltrimethoxysilane was used to improve their compatibility. Lu et al. [19] entrapped polythiourethane with 3-(isocyanatopropyl)triethoxysilane, then mixed with titanium *n*-butoxide and subsequently carried out a sol–gel process to obtain hybrid optical films. Wu [20] employed acrylic acid as a modifier to obtain polycaprolactone-*g*-acrylic acid/TiO_2 hybrid films. Yeh et al. [21] successfully prepared PMMA/TiO_2 using 2-hydroxyethyl methacrylate as coupling agent. We also successfully prepared a series of transparent polyacrylate/TiO_2 hybrid materials with titania sol and acrylic acid or 3-(trimethoxysilyl)propyl methacrylate as function monomers [22–24].

In this paper, we first prepared polyester polyol/titania hybrid resins by use of titania sols from the hydrolysis and condensation of titanium *n*-butoxide under acidic condition, the hybrid resins were then cured by isocyanates to obtain polyester-based polyurethane/titania hybrid films. Since the esterification process usually contains a lot of –COOH and –OH groups and these groups can easily react with –OH or –OR groups at titania during preparing hybrid resins, the titania phase and polyester (polyurethane) phase should have very different interactions from these systems reported previously. Obviously, those interactions can further influence the microstructure, and possibly improve some performances of polyurethanes since polyester-based polyurethanes have been widely used in automotive coatings, coiling coatings, machine coatings, wood coatings and etc.

* Corresponding author. Address: Department of Materials Science and the Advanced Coatings Research Center of China Educational Ministry, Fudan University, Shanghai 200433, People's Republic of China. Tel.: +86 21 65643795; fax: +86 21 65103056.
E-mail address: lxw@fudan.ac.cn (L. Wu).

0032-3861/$ - see front matter © 2006 Elsevier Ltd. All rights reserved.
doi:10.1016/j.polymer.2005.12.073

2. Experimental

2.1. Materials

Titanium *n*-butoxide ($Ti(OBu^n)_4$), acetylacetone (acac), absolute ethanol (99.7%) and hydrochloric acid (37%) were purchased from Sinopharm Group Chemical Reagent Co. Ltd. Phthalic anhydride (98%), adipic acid (99%), 1,4-butanediol (98%), neopentyl glycol (98%) and 4-methyl-2-pentanone (96%) were supplied from Bayer Company. Catalyst: dibutyltin dilaureate (99%) and crosslinking agent: isophorone diisocyanate (IPDI) trimer (solid content: 70%, NCO: 12%) was supplied from Degussa Corporation. All the ingredients were used as received.

2.2. Preparation of titania sols

68.1 mL (0.2 mol) of $Ti(OBu^n)_4$ and 20.5 mL (0.2 mol) of acac (served as ligand) were first dissolved into 40.0 mL of EtOH by stirring at room temperature in a 250 mL three-neck flask, then heated to 500 °C and kept at that temperature for 0.5 h, followed by slowly dropping the solution of 0.01 mol of hydrochloric acid, water (molar ratio of $H_2O/Ti(OBu^n)_4 = 1$, 2, 4 and 8, respectively) and 40.0 mL of EtOH over a period of 0.5 h, and kept at 50 °C under vigorous stirring for another 5 h to form yellow transparent sols.

2.3. Preparation of polyester /titania hybrid resins

Polyester polyol resin was synthesized in a 500 mL round-bottomed flask equipped with a mechanical stirrer, a thermometer with a temperature controller, a N_2 inlet, a Graham condenser and a heating mantle. Pathalic anhydride, adipic acid, neopentyl glocyl and 1,4-butanediol with the molar ratio of 1:4.95:1.36:6.98 were charged into the flask and heated to around 120 °C at a slow stream of N_2, then 0.05 wt% of dibutyltin dilaurate based on the total weight of monomers was added as the catalyst. The reaction was carried out at 165 °C for 4 h.

For polyester/titania hybrid resins, titania sol was mixed with the monomers, then the condensation polymerization was carried out according to the process as described above.

2.4. Preparation of polyurethane/titania hybrid films

The polyester/titania hybrid resins were mixed with IPDI trimer based on the molar ratio of NCO/OH = 1.1:1 and solid content was adjusted to 60 wt% by adding 4-methyl-2-pentanone at room temperature, then 0.05 wt% of dibutyltin dilaurate based on the total weight of the hybrid resin and IPDI

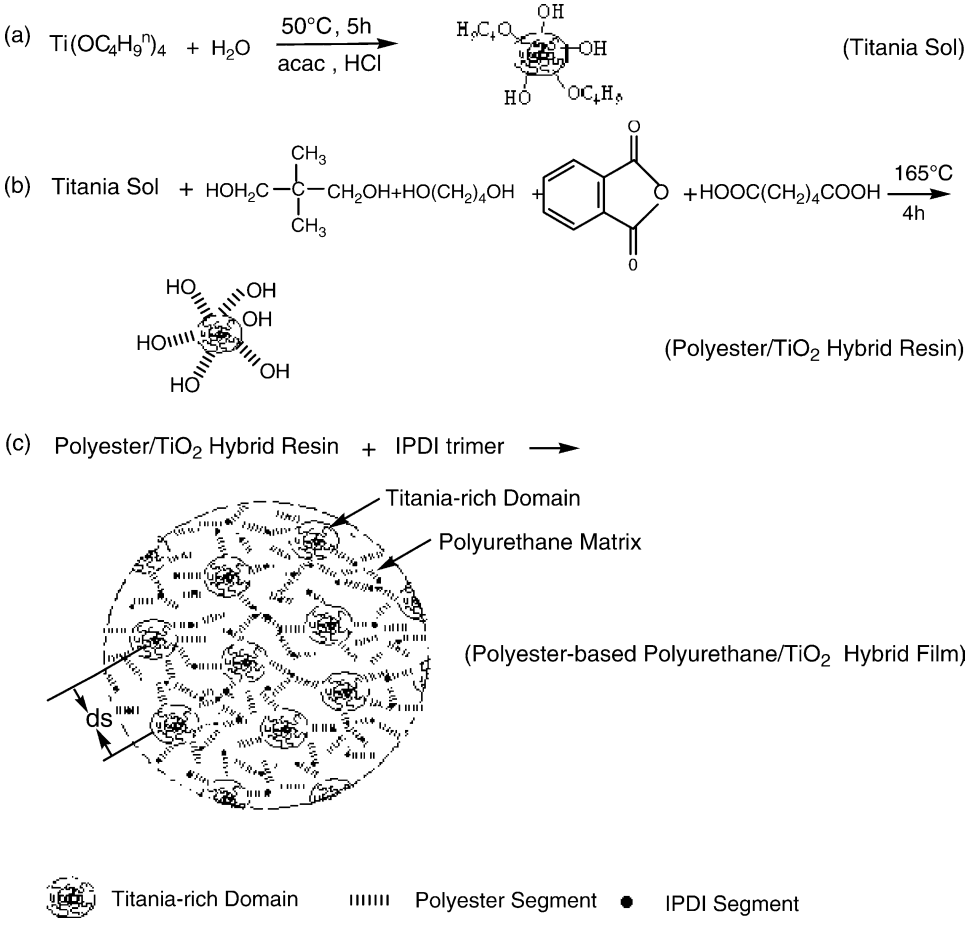

Fig. 1. The schematic diagram of the reaction processes for the preparation of (a) titania sol; (b) polyester/titania hybrid resin; (c) polyurethane/titania hybrid film.

trimer on solid was mixed thoroughly with the solution. The polyurethane/titania hybrid films with ~45 μm thickness were prepared by casting the above solutions onto clear glass substrates, then cured at room temperature for a week and further at 100 °C for 0.5 h before SAXS and DMA measurements. For UV–vis spectroscopy analysis, approximately ~20 μm thick films were prepared via casting the above solutions onto the quartz glass substrates and curing in the same way.

The detailed schematic diagram of the reaction process is displayed in Fig. 1.

All polyurethane/titania hybrid samples are labeled as PUT*a*-*b*, where PU means polyurethane, T*a* indicates the different titania sols, *a* represents the molar ratio of H_2O/Ti(OBu^n)$_4$ and *b* the theoretical titania content in polyester/titania hybrid resin. For an example, the sample PUT2-3 indicates the polyurethane/titania hybrid film is obtained from polyester/titania hybrid resin containing 3–wt% T2 titania sol.

2.5. Characterization

2.5.1. Viscosity measurement

The viscosity of polyester/titania hybrid resins were determined by a NDJ-1A rheoviscometer (Shanghai Shengdi Technology Development Corporation, China) at 20±1 °C.

2.5.2. SAXS analysis

SAXS analyses were performed on a PW 1700 X-ray scattering instrument (Philips Company, Holland) using copper radiation with $\lambda = 0.154$ nm and pinhole collimation of the incident beam. Background collection was performed under the same conditions as the sample data collection. The background counts were scaled and removed from the scattering beam.

2.5.3. AFM observation

AFM topographic images were obtained using Multimode Nanoscope β instrument (Digital Instrument Inc., USA) with noncontact tapping mode with a silica probe (NSC 11) and a frequency of 463 kHz. The roughness analysis was performed on the dimensions of 2×2 μm^2. The average surface roughness (Ra) and root mean square roughness value (Rms) were obtained by averaging the results from five AFM images.

2.5.4. DMA measurement

Dynamic mechanical analysis was carried out on DMA 242 (NETZSCH Inc., Germany). The samples were quickly cooled to −50 °C and equilibrated at that temperature for 3 min, then heated to 120 °C at a frequency of 1 Hz with a constant heating rate of 5 °C/min under nitrogen atmosphere.

2.5.5. Tensile property

Tensile properties were acquired by an Instron DXLL 1000–20000 machine (Shanghai, China). The specimens for tensile tests were dumbbell cut from the molded polymer films according to Die C of ASTM-D412, and carried out at a crosshead speed of 200 mm/min. A 20 mm benchmark and the original cross-sectional area were utilized to calculate their tensile properties. The tensile strength, tensile modulus and elongation at break were automatically calculated by the computer connected to the Instron. The average of at least five measurements for each sample was reported.

2.5.6. Abrasion resistance

Abrasion resistance was determined according to national standard of China GB1768-79. The coated round glass boards were rubbed for 200 cycles by 120# rubber abrasive wheel under 1 kg load. The abrasion resistance was evaluated from the average weight loss of five parallel tests.

2.5.7. Macro-hardness

Macro-hardness of the coats was determined using a pendulum hardness tester (BYK Gardner, Germany). The time swinging from 6 to 2° for the pendulum on the glass with and without polymer hybrid coats were named as t and t_0, respectively. The ratio of t/t_0 was regarded as the macro-hardness.

2.5.8. UV–vis spectra

The absorbance and transmittance spectra of the hybrid films in the range of 200–700 nm wavelength light were determined with a UV–vis spectrophotometer (UV-3000, Hitachi, Japan) at a scanning speed of 300 nm/min.

3. Results and discussion

3.1. Viscosity of polyester/titania hybrid resins

The viscosity of polyester hybrid resins can reflect the interactions between the components of the system. Fig. 2 shows the typical viscosity curves of polyester/titania hybrid resins as a function of titania content. It was found that the viscosity obviously increased as titania content increased, especially at high titania content. This was because the titania obtained under acid condition was primarily composed of network structure with large amount of –OH and –OC_4H_9

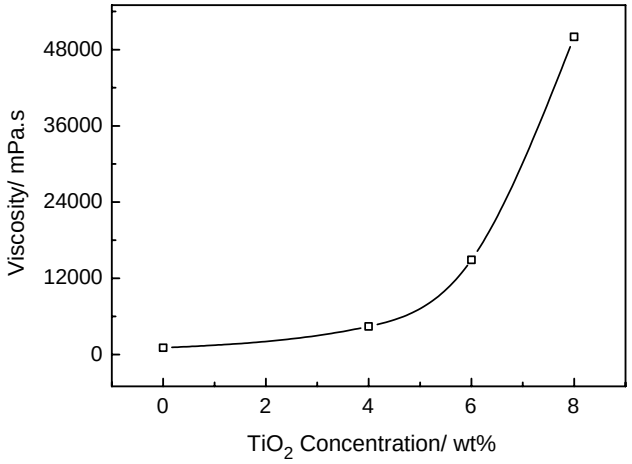

Fig. 2. Typical viscosity variation of polyester/titania hybrid resins with titania content.

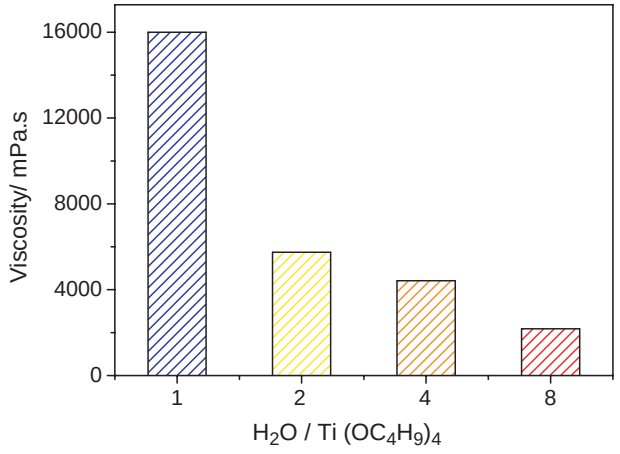

Fig. 3. Effect of the types of titania sol on the viscosity of polyester/titania hybrid resin.

groups [24]. When it was embedded into polyester resin via in situ method, the condition of esterification reaction could further make some reactions between titania networks themselves or between titania networks and monomers or oligomers with –OH or –COOH groups. Thus the titania phase could act as physical or chemical crosslinking points, increasing the viscosity of polyester resin. Obviously, the more the titania was introduced, the more the crosslinking points formed, the higher the viscosity was.

The effect of the types of titania sols on the viscosity of polyester/titania hybrid resins was displayed in Fig. 3. It could be seen that titania sols produced at less water content caused much higher viscosity of hybrid resin. This could be explained as follows: in the sol–gel process of $Ti(OBu^n)_4$, less water meant more $–OC_4H_9$ groups remaining in the corresponding titania networks [23,24], which availed forming more chemical interactions especially between titania networks and polyester segments through the condensation reaction of the $–OC_4H_9$ groups and –OH groups, increasing the viscosity of the system.

3.2. Microstructure of polyurethane/titania hybrid films by SAXS

The microstructure of the titania phase in the polyurethane/titania hybrid films was characterized by SAXS through two parameters: radius of gyration (R_g) and fractal dimension (D), measures of the mean-square distance of the scattering centers within inorganic domains from the center of gravity and the compactness of inorganic domains, respectively. R_g can be calculated from the slope in the linear region of a plot of $\ln(I(q))$ versus q^2, according to Guinier's relation[25,26]:

$$I(q) \propto \exp(-q^2 R_g^2/3) \quad (1)$$

where $I(q)$ is scattering intensity, scattering vector $q=(4\pi/\lambda)\sin(2\theta/2)$, 2θ is the scattering angle and λ is the wavelength of the beam. D can be obtained from Porod plot, namely a log–log plot of SAXS data. The slope of the linear region in the Porod plot is called the Porod slope (P). For $-3<P<0$, objects are considered as mass fractal in three-dimension with fractal dimension (D_m) ranging from 0 to 3 ($P=-D_m$), while for $-4<P<-3$, objects are surface fractal with fractal dimension (D_s) ranging from 2 to 3 ($P=D_s-6$) [25,27].

Fig. 4(a) demonstrated the SAXS profiles of the pure polyurethane and the hybrid films with different content T4 as examples. The pure polyurethane had almost zero scattering intensity. However, all the hybrid films exhibited high scattering intensity resulting from the relative electron density difference between polyurethane and titania-rich phase. Moreover, the scattering intensity increased with higher titania

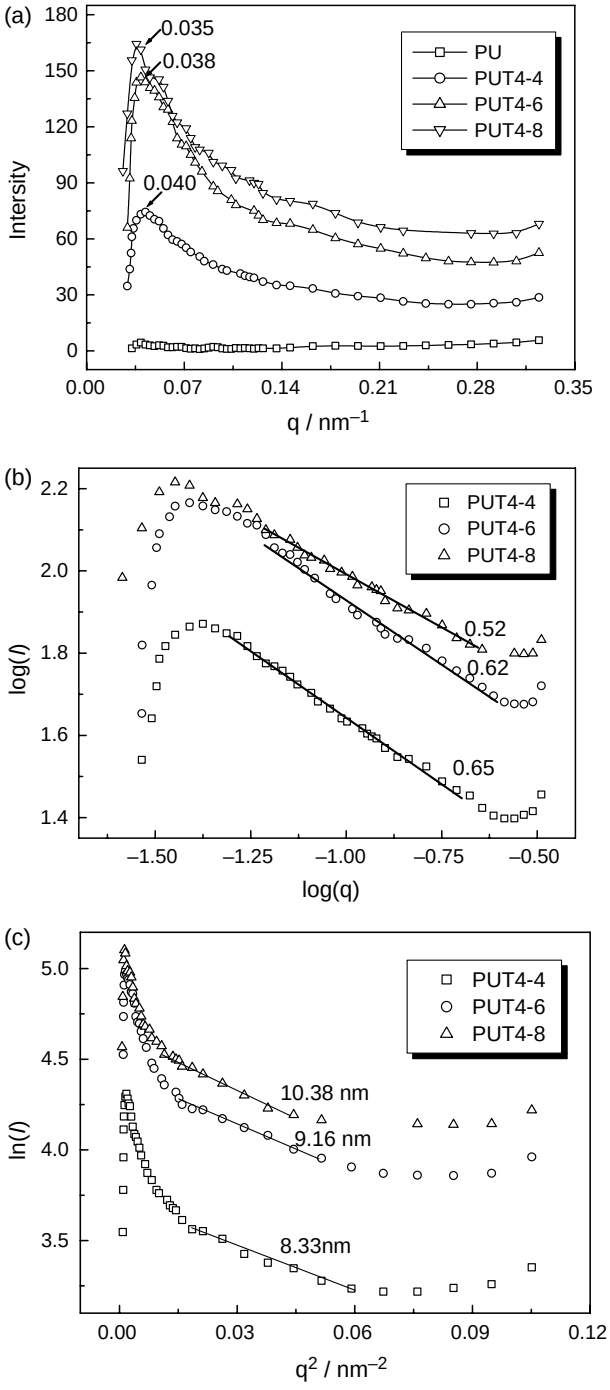

Fig. 4. SAXS profiles of PUT4-4, PUT4-6 and PU4-8 (a) and their corresponding Porod plots (b) and Guinier plots (c).

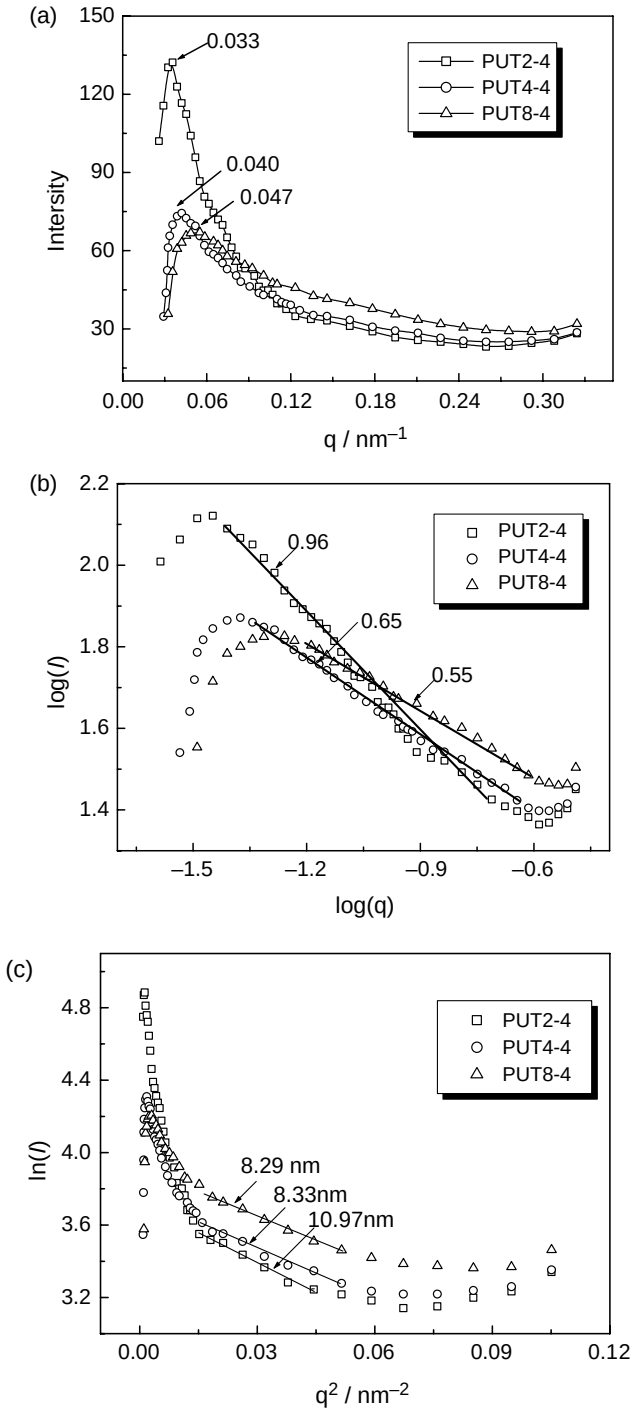

Fig. 5. SAXS profiles of PUT2-4, PUT4-4 and PUT8-4 (a) and their corresponding Porod plots (b) and Guinier plots (c).

content, indicating an increase in phase separation or a decrease in miscibility [26]. Meanwhile, a scattering peak was also observed for all hybrid films, which meant the existence of the short-range periodicity of titania-rich domains. As we know, the scattering peaks could also be used to estimate the average distance between the titania-rich domains by calculating the interdomain spacing $d_s = 2\pi/q_{max}$, where q_{max} was the scattering vector at the peak maximum [28]. As the titania content increased, the q_{max} values decreased from 0.040 nm^{-1} (PUT4-4) to 0.035 nm^{-1} (PUT4-8), corresponding d_s values increased from 157 to 179 nm, indicating a slight increase of the distance between the titania-rich domains. Fig. 4(b) and (c) manifested the corresponding Guinier and Porod plots showing linear regions. The radius of gyration (R_g) and fractal dimension (D) calculated from the linear region were also given in the figures. All of the D values of hybrid films were lower than 1.0, see Fig. 4(b), suggesting titania-rich domains with mass fractal dimension and very open structure. As titania content increased, D values decreased from 0.65 (PUT4-4) to 0.52 (PUT4-8), corresponding R_g values increased from 8.33 to 10.38 nm, see Fig. 3(c), indicating that the titania networks interacted with each other through chemical reaction or hydrogen bonding during esterification process, forming looser but bigger titania-rich domains in hybrid films at higher titania content.

When titania sols changed from T8 to T4 and T2, all of the SAXS profiles of hybrid films revealed a sharp scattering peak, as displayed in Fig. 5, and their scattering density increased correspondingly, indicating that there were titania-rich domains with short range periodicity structure in all the hybrid films, and their extent of phase separation increased while miscibility decreased as water content decreased in the sol–gel process. The q_{max} values decreased from 0.047 nm^{-1} (PUT8-4) to 0.033 nm^{-1} (PUT2-4), see Fig. 5(a), corresponding d_s values increased from 133 to 190 nm, D values increased from 0.55 to 0.96 while R_g from 8.29 to 10.97 nm, see Fig. 5(b) and (c), indicating the titania-rich domains became compacter and larger while distance between them became longer in hybrid films as water content decreased in the preparation of titania sol. Although less water was in favor of the formation of titania networks with looser even nearly linear structure (such as T2) in the preparation of titania sol, these titania networks with more –OC_4H_9 groups remained not only more easily chemical bonded with polyester oligomers or monomers but also more easily condensed between these embedded titania networks themselves in the environment of esterification, so the new formed titania-rich domains in the hybrid have both much compacter and larger microstructure.

3.3. Morphology of the hybrid films by AFM

The three-dimension AFM images of the pure polyurethane and hybrid films embedded by different titania sols were displayed in Fig. 6, corresponding surface roughness values were summarized in Table 1. No obvious agglomerates were observed in all of the surfaces of hybrid films compared with the pure polyurethane, which meant a good miscibility and the titania-rich domains dispersed into polyurethane in nano-scale. As the introducing titania sols changed from T2 to T4 and T8, no obvious changes appeared for the corresponding hybrid films shown in Fig. 6(b)–(d), respectively, but corresponding Rms or Ra values decreased slightly as Table 1 revealed, which might be related to the existence of titania-rich domains in hybrids with smaller and softer structure as indicated by SAXS.

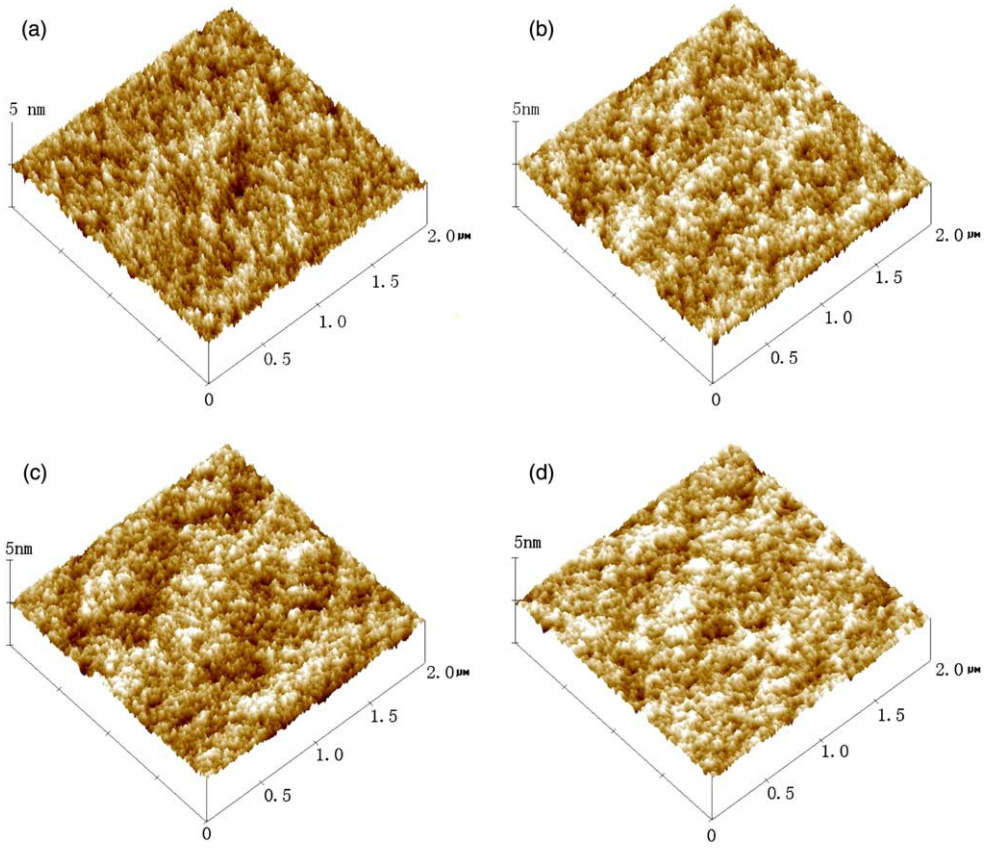

Fig. 6. AFM images of pure polyurethane (a) and typical polyurethane hybrid films PUT2-4 (b), PUT4-4 (c) and PUT8-4 (d), respectively.

3.4. DMA analysis

The storage modulus (E') and tan δ as a function of temperature for the pure polyurethane and the hybrid films were shown in Figs. 7 and 8. The temperature at the peak of the tan δ curve is defined as the glass transition temperature (T_g) and the height of the tan δ peak regarded as relaxation strength. Meanwhile, the crosslinking density (ν_e) of the hybrid films can be calculated according to the following equation [29]

$$\nu_e = \frac{E'}{(3RT)} \quad (T \gg T_g) \tag{2}$$

where R is the gas constant and T is the absolute temperature. The equation is effective only when T is more than 50 °C above T_g. Herein, the E' value at 130 °C was adopted. All of the corresponding data were summarized in Table 2.

Fig. 7 showed that the hybrid films had higher E' value than pure polyurethane, and the E' value gradually increased with increasing titania content. Correspondingly, the tan δ peaks became broader and shifted to higher temperature. The data in Table 2 further revealed that the T_g increased from 61.1 to 84.2 °C and the crosslinking density from 1.55 to 6.17 mol/m^3 as the titania content in hybrid resin changed from 4 to 8 wt% (see the samples PUT4-4, PUT4-6 and PUT4-8). More polyester segments bonded with titania networks should be responsible for the higher crosslink density and higher T_g of the hybrid films at higher titania content, which agreed with the variety of viscosity with titania content. Meanwhile, the broader tan δ peak and lower relaxation strength of the hybrid film with higher titania content also indicated that more organic segments were chemically bonded or entrapped within inorganic domains [30].

Fig. 8 demonstrated that the E' of polyurethane/titania hybrid film increased in the order of PUT8-4 < PUT4-4 < PUT2-4, and the tan δ peak became broader and shifted to higher temperature correspondingly. The data in Table 1 showed that the corresponding T_g increased from 56.8 to 64.2 °C and the crosslinking density from 1.06×10^{-2} to 2.01×10^{-2} mol/m^3, indicating more $-OC_4H_9$ groups remaining in the titania sol caused more interaction between titania networks and polyester segments.

3.5. Mechanical properties of hybrid coats

Table 3 summarized the tensile properties, abrasion resistance and macro-hardness of the polyester-based polyurethane/titania hybrid coats. Comparing with the pure polyurethane, the hybrid coats had higher tensile strength,

Table 1
Rms and Ra of pure polyurethane and corresponding hybrid films

Sample	Rms (nm)	Ra (nm)
PU	0.242	0.182
PUT2-4	0.276	0.221
PUT4-4	0.261	0.208
PUT8-4	0.251	0.184

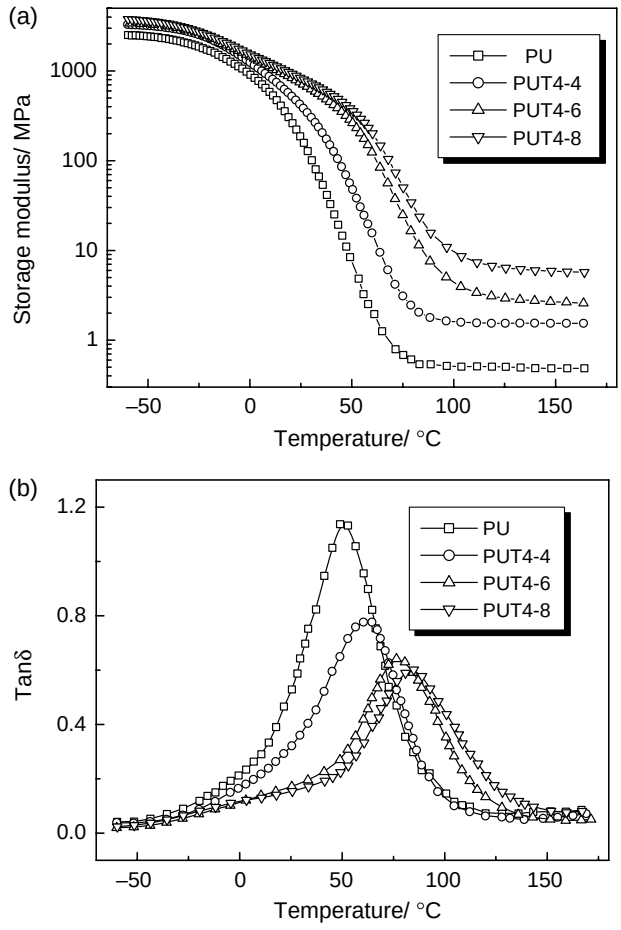

Fig. 7. Effect of the titania content on the E' (a) and tan δ (b) curves of the hybrid films.

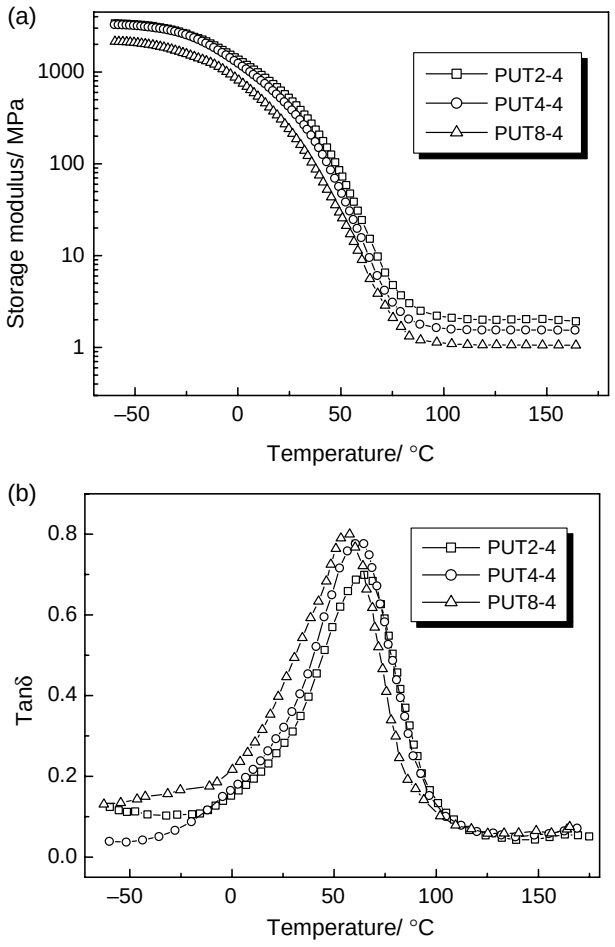

Fig. 8. Effect of the titania sols prepared at different water content on the E' (a) and tan δ (b) curves of the hybrid films.

modulus, abrasion resistance and hardness except for elongation at break. Moreover, the tensile strength, modulus, abrasion resistance and hardness obviously increased as the titania content increased (see the samples PU4-4, PU4-6 and PU4-8). The types of titania sol also influenced the tensile properties of the hybrid films. The tensile strength, modulus, abrasion resistance and hardness increased in the order of PUT8-4 < PUT4-4 < PUT2-4, in consistent with the DMA results, suggesting that more interaction between organic matrix and titania phase caused better mechanical strength, abrasion resistance and hardness.

3.6. Optical properties

Fig. 9 shows the UV–vis absorbance and transmittance spectra of pure polyurethane and the typical hybrid films. For the pure polyurethane film, there was almost no absorption in the range of 290–400 nm wavelength. When titania was introduced into the polymers, obvious absorbance in the UV region was observed, and this absorbance increased significantly with increasing titania content. As we knew, titania bulk material had a band-gap of 3.2 eV (absorption edge at 387.5 nm) [31], the band gap shift $\geq E_g$ dependence of the radius R was [32]:

Table 2
DMA data for the pure polyurethane and the polyurethane/titania hybrid films

Sample	E' (MPa)	$\nu_e \times 10^2$ (mol/m^3)	T_g (°C)	Relaxation strength
PU	0.49	0.49	50.4	1.15
PUT2-4	2.01	2.01	64.2	0.69
PUT4-4	1.55	1.55	61.1	0.78
PUT8-4	1.06	1.06	56.8	0.81
PUT4-6	2.83	2.82	76.3	0.64
PUT4-8	6.17	6.17	84.2	0.59

Table 3
Tensile properties, abrasion resistance and macro-hardness of polyurethane and polyurethane/titania hybrid coats

Sample	Tensile strength (MPa)	Elongation-at-break (%)	Tensile modulus (MPa)	Weight loss (g)	Macro-hardness
PU	8.2	178	91	0.025	0.20
PUT4-4	14.5	125	167	0.017	0.31
PUT4-6	17.5	83	217	0.015	0.37
PUT4-8	26.8	56	278	0.013	0.42
PUT2-4	18.3	127	232	0.016	0.32
PUT8-4	11.2	132	143	0.021	0.24

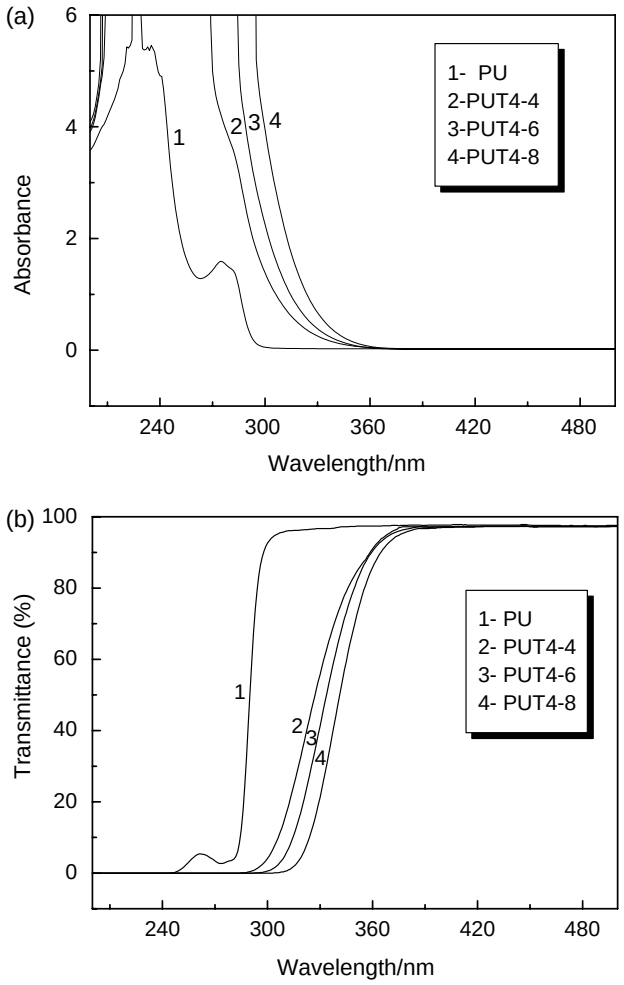

Fig. 9. Effect of titania content on the UV–vis absorbance (a) and transmittance (b) spectra of the typical polyurethane/titania hybrid films.

$$\Delta E_g = \frac{h^2}{8MR^2} - \frac{1.8e^2}{\varepsilon R} \quad (3)$$

where h is Planck's constant, M is the reduced effective mass of the electron, e is the electron charge, ε is the dielectric constant of the solid. The first term, proportional to R^{-2}, is the shift to higher energy gap due to quantum localization, while the second term, proportional to R^{-1}, is the shift to lower energy gap due to the electrostatic interaction between the electron and the hole. When the size of titania was small enough, especially lower than 10 nm, the band gap value increased dramatically with the decrease of titania size, leading to the blue-shift of absorption edge for titania phase due to a quantum size effect [33]. Similar to the tendency of titania matrix with rutile or anatase structure, Fig. 9 also revealed a blue-shift of absorption edge for the titania phase with amorphous and open network structure in hybrid. All of the transmittance spectra of the hybrid films exhibited excellent optical transparence in the visible range (400–700 nm), which was due to the smaller size of titania phases in hybrid than that of visible light. The transmittance in the UV region decreased with increasing titania content in the hybrid films, suggesting that the polyester-based polyurethane/titania hybrid films could improve the UV shielding property of the polymer without decreasing the transparence.

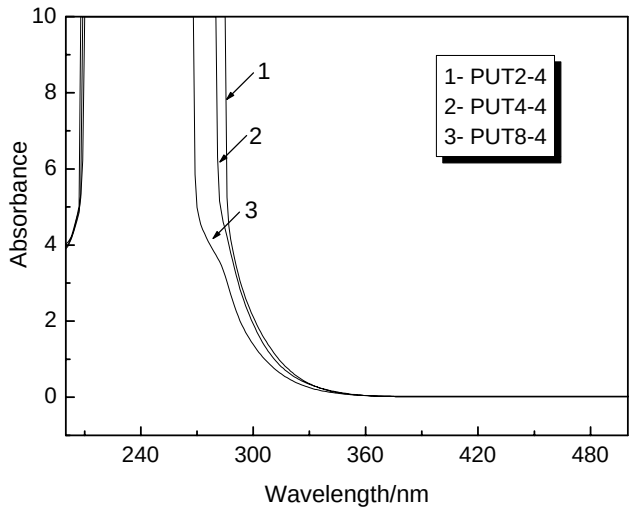

Fig. 10. Effect of the types of titania sol on the UV–vis absorbance spectra of the polyurethane/titania hybrid films.

Fig. 10 showed the effect of the type of titania sol on the UV–vis absorbance spectra of the hybrid films. All of the hybrid films had strong absorbance in the UV region and good transparence. As the titania sol changed from T2 to T4 and T8, the UV absorbance of the corresponding hybrid film gradually reduced, probably because of looser and smaller titania-rich domains in hybrid film obtained at more water content as SAXS measurements.

4. Conclusions

Transparent polyester-based polyurethane/titania hybrid films were successfully prepared via in situ method using titania sol from the hydrolysis and condensation of titanium *n*-butoxide under acidic condition. The more the titania, or the titania produced at less water content was embedded, the higher viscosity of hybrid resin was. SAXS measurements indicated the titania-rich domains in the hybrid films had mass fractal dimension and very open network structure. The more titania was embedded, the larger and looser the titania phase in the hybrid film was, while the titania obtained by less water, the larger and denser the titania phase in the hybrid film was. The more titania, or the titania from less water was introduced, the higher the T_g, modulus, tensile strength, abrasion resistance, hardness and UV absorbance of the hybrid films were. This meant that the transparent polyester-based polyurethane/titania hybrid films with improved UV-shielding and mechanical properties could be prepared by this approach.

Acknowledgements

We thank National '863' Foundation, Shanghai Special Nano Foundation, the Key Project of China Educational Ministry, the Doctoral Foundation of University and Trans-century Outstanding Talented Person Foundation of

China Educational Ministry for financial support for this research.

References

[1] Vogel R, Mreredith P, Kartini I, Harvey M, Riches JD, Bishop A, et al. Chem Phys Chem 2003;4:595.
[2] Frach P, Gloss D, Goedicke K, Fahland M, Gnehr WM. Thin Solid Films 2003;445:251.
[3] Francioso L, Presicce DS, Taurino AM, Rella R, Siciliano P, Ficarella A. Sens Actuators, B-Chem 2003;95:66.
[4] Du XY, Wang Y, Mu YY, Gui LL, Wang P, Tang YQ. Chem Mater 2002; 14:3953.
[5] Hansel H, Zettl H, Krausch G, Kisselev R, Thelakkat M, Schmidt HW. Adv Mater 2003;15:2056.
[6] Kron G, Rau U, Werner JHJ. Phys Chem B 2003;107:3258.
[7] Bosc F, Ayral A, Albouy PA, Guizard C. Chem Mater 2003;15:2463.
[8] Nakamura R, Imanishi A, Murkoshi K, Nakato YJ. Am Chem Soc 2003; 125:7443.
[9] Chen WC, Liu WC, Wu PT, Chen PF. Mater Chem Phys 2004;83:71.
[10] Miura S, Naito H, Kanemitsu Y, Matsuura Y, Matsukawa K, Inoue H. Thin Solid Films 2003;438–439:253.
[11] Perrin FX, Nguyen V, Vernet JL. Polymer 2002;43:6159.
[12] Chiang PC, Whang WT, Tsai MH, Wu SC. Thin Solid Films 2004;447–448:359.
[13] Liu L, Lu QH, Yin J, Zhu ZK, Pan DC, Wang ZG. Mater Sci Eng C 2002; 22:61.
[14] Que WX, Hu X. J Sol–Gel Sci Technol 2003;28:319.
[15] Agag T, Tsuchiya H, Takeichi T. Polymer 2004;23:7903.
[16] Perrin FX, Nguyen V, Vernet JL. Polymer 2002;23:6159.
[17] Lee LH, Chen WC. Chem Mater 2001;13:1137.
[18] Sarwar MI, Ahmad Z. Eur Polym J 2000;36:89.
[19] Lu CL, Cui ZC, Guan C, Guan JQ, Yang B, Shen JC. Macromol Mater Eng 2003;9:288.
[20] Wu CS. J Appl Polym Sci 2004;92:1749.
[21] Yeh JM, Weng CJ, Huang KY, Huang HY, Yu YH, Yin CH. J Appl Polym Sci 2004;94:400.
[22] Xiong MN, You B, Zhou SX, Wu LM. Polymer 2004;45:2967.
[23] Xiong MN, Zhou SX, Wu LM, Wang B, Yang L. Polymer 2004;45: 8127.
[24] Xiong MN, Zhou SX, You B, Gu GX, Wu LM. J Polym Sci, Part B: Polym Phys 2004;42:3682.
[25] Betrabet CS, Wilkes GL. Chem Mater 1995;7:535.
[26] Habsuda J, Simon GP, Cheng YB. Polymer 2002;43:4627.
[27] Hajji P, David L, Gerard JF, Pascault JP, Vigier G. J Polym Sci, Part B: Polym Phys 1999;37:3172.
[28] Dahmouche K, Santilli CV, Pulcinelli SH, Craievich AF. J Phys Chem 1999;103:4937.
[29] Ni H, Skaja AD, Soucek MD. Prog Org Coat 2000;40:175.
[30] Tai H, Sargienko A, Silverstein MS. Polymer 2001;42:4473.
[31] Liu YJ, Claus RO. J Am Chem Soc 1997;119:5273.
[32] Sorek Y, Reisfeld R, Weiss AM. Chem Phys Lett 1995;244:371.
[33] Anpo M, Shima T, Kodama S, Kubokama Y. J Phys Chem 1987;91: 4305.